



Original Article

Phospholipid and Triglyceride keep vortex-dispersed sulfur mustard analog as undissolved droplets which induce necrosis from nearby cells via declining mitochondrial membrane potential

Feng Ye¹, Guorong Dan¹, Qinya Zeng², Mingliang Chen¹, Yuanpeng Zhao¹, Jin Cheng¹, Yan Sai¹, Jiqing Zhao¹ and Zhongmin Zou¹

¹Department of Chemical Defense, School of Military Preventive Medicine, Army Medical University, Chongqing, 400038, China

²Department of Anesthesiology, Second Affiliated Hospital, Army Medical University, Chongqing, 400037, China

(Received November 11, 2019; Accepted November 27, 2019)

ABSTRACT — SM (Sulfur mustard) is an oily, hydrophobic, and lipophilic chemical agent that damages cells with intricate patterns. CEES (2-chloroethyl ethyl sulfide soluble) is a standard SM analog commonly employed in the toxicity mechanism study. To obtain ideal results *in vitro*, researchers should disperse CEES well in the medium, avoiding the presence of undissolved droplets. However, such a purpose is not easy to reach under the conventional solution preparation, and the information about droplet formation and function is little available. Here, we showed that phospholipid and triglyceride, two essential components of serum lipids, could prevent CEES from dissolving in water after vortex, which kept partial CEES as small droplets. By detecting CEES level, we proved that residual droplets slowed CEES hydrolysis and conversion. Under the microscope, CEES droplets were observed to degrade and diffuse with time to induce the necrosis and mitochondrial membrane potential decline from nearby cells. In conclusion, the damage pattern of CEES droplets is quite different from that of dissolved CEES, and a low level of phospholipid and triglyceride is beneficial for preventing droplets formation in preparing CEES solution.

Key words: CEES droplets, Phospholipid, Triglyceride, Necrosis, Mitochondrial membrane potential

INTRODUCTION

Sulfur mustard (SM), an oily and hydrophobic agent, was used as a chemical warfare agent in World War I, the Iran–Iraq War 1980–1988, and the recent Syria civil war (Sezigen *et al.*, 2019). SM can severely damage tissues or organs due to the result of an acute or long term effect (Balali-Mood *et al.*, 2019; Khazdair and Boskabady, 2019). The severe damage by SM is hard to repair since the toxicity mechanism of SM is complex and not fully known (Panahi *et al.*, 2018; Rose *et al.*, 2018; Shakarjian *et al.*, 2010). Its relative ease of production and stockpiling, together with its multiple incapacitating health

effects, making SM a continuous threat.

In vitro study on the sophisticated cell system is a meaningful way to explore the mechanism of SM toxicity (Allon *et al.*, 2010; Deppe *et al.*, 2016; Steinritz *et al.*, 2013). Before application, SM is freshly stocked in an organic solvent, which is further diluted and vortexed in the medium as a working solution. Once dissolving in water, SM can dissociate its chlorine atom to an active sulfonium ion which damage cells, such as DNA alkylation, enzyme inactivation, and metabolic disturbance. The active pattern of SM is unstable and can quickly convert to other derivatives, which are less vesicant and toxic (Noort *et al.*, 2002; Price and Bullitt, 1947). To get the

required level, SM should be well-dispersed to prevent the existence of residual droplets *in vitro* experiments as much as possible.

The commercial serum is an essential supplement for cell culture. In the previous study, we found that residual droplets of CEES (2-chloroethyl ethyl sulfide, an analog of SM) were hard to be avoided when diluting CEES in medium containing serum. Due to the lack of information about droplets formation, character, and cytotoxicity, until now, which components in serum may promote CEES droplets formation is still unknown. Since lipids are essential components in serum, and CEES is a known lipophilic agent, we assumed that serum lipids, such as Phospholipid (PL, solid) and Triglyceride (TG, oil), may participate in the formation of CEES droplets.

In this study, we provided the evidence that either individual or complex of PL and TG could facilitate the formation of CEES droplets that can induce necrosis from nearby cells by declining mitochondrial membrane potential (MMP). To our knowledge, this is the first report focusing on CEES droplets *in vitro* condition, which may have implications for *in vitro* study.

MATERIALS AND METHODS

Reagents and cellular treatments

CEES (Purity > 97%, CAS number: 693-07-2) was obtained from Sigma (St. Louis, MO, USA). Potassium thioacetate (PTA) was obtained from Shanghai Dipper Chemicals (Analytical grade, purity > 98%). All other reagents were of analytical purity.

Human pulmonary bronchial cells (HBE) were obtained from Xiangf bio (Shanghai, China). Cells were cultured in MEM (HyClone, Logan, UT, USA) supplemented with 10% fetal bovine serum (Kang Yuan Biology, Tianjin, China), 100 U/mL penicillin and 100 U/mL streptomycin (Beyotime, Shanghai, China). The cells were maintained in a humidified incubator at 37°C and 5% CO₂. One day prior CEES exposure, cells were digested and placed on a culture plate to reach over 90% confluence for the next treatment.

Prior to CEES application, a 1 M stock solution of CEES in dimethyl sulfoxide (DMSO) was freshly prepared under a fume hood to allow volatile venting agents and kept on ice. CEES was diluted to a final concentration of 0.5 mM with 5-sec vigorous vortex on an oscillator and added into the cell culture plate immediately. The entire procedure was limited within 20 sec, according to the suggestion from another report (Tewari-Singh *et al.*, 2010). After one-hour CEES exposure, the toxic medium was replaced with fresh medium. The percentage of

DMSO did not exceed 0.1% in the culture medium.

CEES droplets formation assay

To explore the correlation between the dilution mediums and CEES droplets formation, we prepared three different mediums containing 1 mg/mL PL (Solarbio, Beijing, China), 1 mg/mL TG (Sigma, USA), or 1 mg/mL PL-TG (0.5 mg/mL PL and 0.5 mg/mL TG), respectively. All mediums were filtered through a 0.45 µm membrane before application. Then, 500 µL CEES solutions (0.5 mM) were freshly prepared and added to each 24-well plate immediately. The amount of CEES droplets was subsequently counted under a microscope.

Mitochondrial membrane potential detection

Cellular MMP was detected using JC-1 probe (Beyotime, China). For *in situ* detection, cells were washed with 0.01 mol/L PBS (PH 7.4) three times and incubated with 1 µg/mL JC-1 probe (diluted in MEM) at 37°C for 20 min. Subsequently, the cells were washed with PBS three times again to remove the free JC-1 probe. Then, under the fluorescence microscopy (Olympus, Tokyo, Japan), fluorescent signals were recorded at the emission wavelength of 529 nm and 590 nm, respectively. The green signal in cells reflected a reduction of MMP, while the red signal reflected a normal MMP.

For calculation, cells were digested and stained with JC-1, as mentioned above. After a sufficient wash with PBS, the fluorescence intensity of cells (1×10^4) was analyzed using FC500 flow cytometry (Beckman, Atlanta, Georgia, USA) under both FL1 and FL3 channels. The cells with MMP decline were separated from normal cells by setting specific gates, which was further analyzed using CXP software (Beckman, USA).

Necrotic cells analysis

To separate the necrotic cells from others, we pursued the Annexin V-PI dual staining kit (KeyGen Biotech, Nanjing, China). In brief, CEES-treated cells (1×10^6) and the control were digested and washed with PBS. After being centrifuged at 1000 g for 5 min, cells were re-suspended with 195 µL of 1×Binding buffer containing 5 µL Annexin V-FITC and incubated for 10-15 min at the dark condition. Then, 5 µL PI was added into the mixture for 5 min incubation. The fluorescence intensity of about 10^4 cells was subsequently measured using FC500 flow cytometry under both FL1 (Annexin V) and FL3 (PI) channels. The percentage of cells with MMP decline was further analyzed using CXP software (Beckman, USA).

For *in situ* detection, cultured cells were washed with PBS three times and incubated with PI as mentioned

above. After that, cells were washed thoroughly with PBS to remove the free probe. The fluorescent signal was detected using fluorescence microscopy at the emission wavelength of 617 nm. The red signal in nuclear reflected the necrotic cells.

CEES level detection

Sample preparation was modified from a published report (Xu *et al.*, 2015). In brief, 1 M stock solution of CEES was diluted into ultra-pure water containing 1 mg/mL PL-TG or not to a final concentration of 0.5 mM, and immediately vortexed in an oscillator for 5 sec in room temperature (24°C). At 0, 3, 9, 30, 60 min after the preparation, an ice-cold 400 μ L acetonitrile was added to each 800 μ L-aliquoted CEES solution and vortexed for 5 sec. Then, a 400 μ L PTA solution (1 mg/mL in water) was added and vortexed for 5 sec. The mixture was subsequently heated at 50°C for 0.5 hr. After been filtered through a 0.45 μ m membrane, the samples were now ready for analysis using the high-performance liquid chromatography-Ultraviolet (HPLC-UV) system.

The analytical separation was performed with an HPLC-UV system (Shimadzu Co, Japan) equipped with SinoChrom ODS-AP C18 column (5 μ m, 250 \times 4.6 mm), and the column temperature was set at 40°C. The mobile phase A was 0.1% formic acid in the water, while the mobile phase B was acetonitrile. The elution gradient started at 20% B for 1 min and linearly increased to 90% B over 5 min, with a flow rate of 1 mL/min. The volume injection was 25 μ L, and UV detection was performed at 240 nm.

Statistical analysis

All data were representatives of at least triplicate independent experiments. The statistical analysis was conducted with one-way analysis of variance and the *t*-test using SPSS 13.0 statistical software (SPSS Inc., Chicago, IL, USA). $P < 0.05$ is considered to be statistically significant.

RESULTS

PL and TG prevented CEES from dissolving in water after vortex, which kept partial CEES as small oily droplets

Firstly, we directly added 1 μ L CEES stock solution (1 M) into a 24-well plate containing 500 μ L MEM medium. Under the microscope, the diameter of undispersed CEES droplets on glass ranged from a few microns to hundreds of microns, which can be easily identified due to their refraction (Fig. 1A). The vigorous vortex could

disperse CEES solution well with no significant droplets present in the control group, while 1 mg/mL PL, TG or PL-TG could block vortex-dissolved CEES, which kept partial toxicant as small CEES droplets. The number of CEES droplets was counted, and the average amount of CEES droplets induced by these chemicals is TG<PL<PL-TG (Fig. 1B). The feature of CEES solution in control and PL-TG group under the microscopy was shown (Fig. 1C).

PL-TG partially slowed CEES conversion after vortex

It is known that CEES can quickly hydrolyze once it dissolving in water. Thus, we assumed that PL-TG-promoted CEES droplets formation could partially block this process. To measure CEES level, we established a method based on the HPLC-UV system, which detected the derivative of CEES and potassium thioacetate (PTA). The principle of the chemical reaction, as shown in Fig. 2A. After separation, the CEES derivative was detected at 15 min, with the maximum absorbance at 240 nm (Fig. 2, A and C). The standard curve showed that CEES level from 0.03 mM to 1.0 mM correlated well with the peak area, indicating the feasibility of CEES quantification (Fig. 2B). Additionally, we detected that only 31.2%, 18.3%, and 5.3% of CEES remained in control medium at 3, 9, and 30 min after vortex, indicating a rapid conversion of the dissolved CEES. CEES level in the PL-TG group was significantly higher than that in the control group after vortex (46.1% at 3 min, 27.6% at 9 min, both $P < 0.05$) (Fig. 2D), which further insisted the surmise that PL-TG could block the solubility of CEES.

CEES droplets focally damaged nearby cells

We noticed that PL-TG prevented CEES hydrolysis early after vortex (3 or 9 min) but not latter (30 or 60 min), suggesting that CEES droplets should degrade and hydrolyze with time. Under the microscope, we observed that the feature of the CEES droplets went on change once it stayed on the glass. Different from its original feature at 0 min, CEES droplets changed to be irregular with dim refraction 60 min later (Fig. 3A). In cultured cells, most cells around CEES droplets rounded up, detached or debris obviously, indicating that CEES droplets focally damaged nearby cells (Fig. 3B).

CEES droplets increased the percentage of necrotic cells

In situ study, cells nearby CEES droplets exhibited weak light refraction, but intense PI staining. Meanwhile, the cells outside the damaged area were little affected (Fig. 4A). Additionally, flow cytometry showed that the percentage of necrotic cells in the PL-TG group is high-

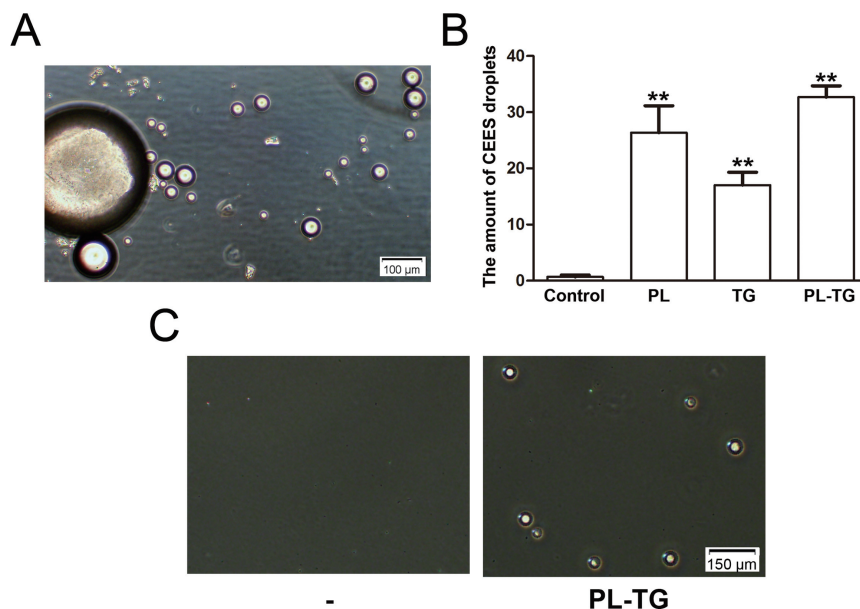


Fig. 1. Effects of PL and TG on CEES droplets formation. (A) 1 μL stock solution of CEES (1 M in DMSO) was directly added into 24-well plate (pre-covered with slide) pre-filled with 500 μL MEM medium, the feature of CEES droplets under a microscope was shown. (B) 500 μL 0.5 mM CEES was freshly prepared in MEM containing 1 mg/mL PL, TG, PL-TG or not. After 5 sec vortex, the toxic medium was immediately added on each glass from 24-well plate. The number of CEES droplets (diameter > 10 μm) was subsequently counted, **, $P < 0.01$, compared with the control group ($n=6$). (C) The feature of CEES solution containing PL-TG or not on glass was shown.

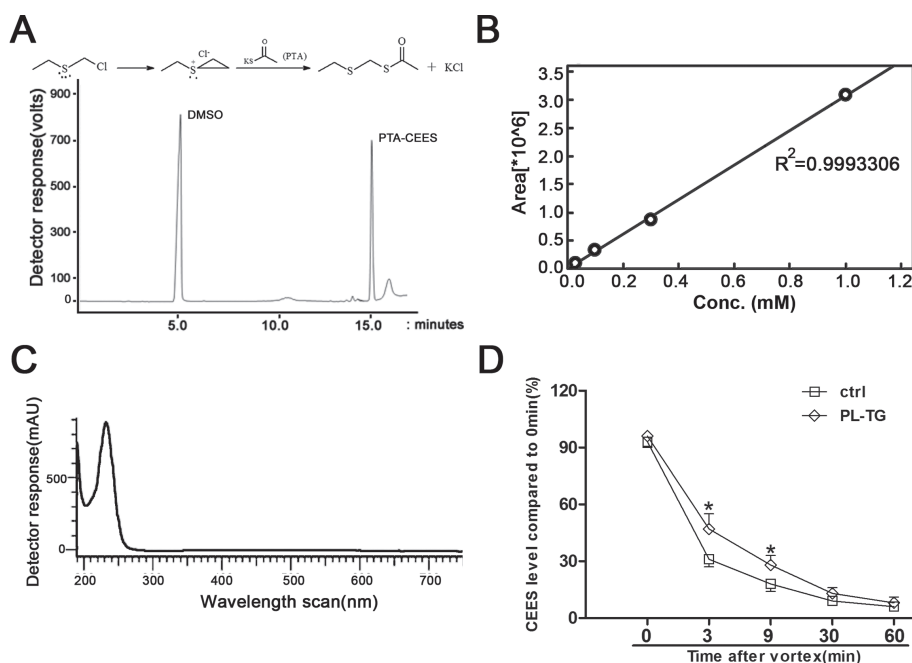


Fig. 2. Measurement of CEES using HPLC. (A) The spectrum of CEES derivative detected using an HPLC-UV system at 240 nm. The principle of derivative reaction between PTA and CEES was shown above. (B) The linear relationship between CEES derivative concentration and peak area. (C) The absorbance value of CEES derivative after 200 to 800 nm wavelength scanning. (D) Analysis of the hydrolysis rate of CEES (0.5 mM) in water containing 1 mg/mL PL-TG or not. *, $P < 0.05$; compared to the control group at the same time point ($n=4$).

Formation, degradation, and toxicity of sulfur mustard analog droplets

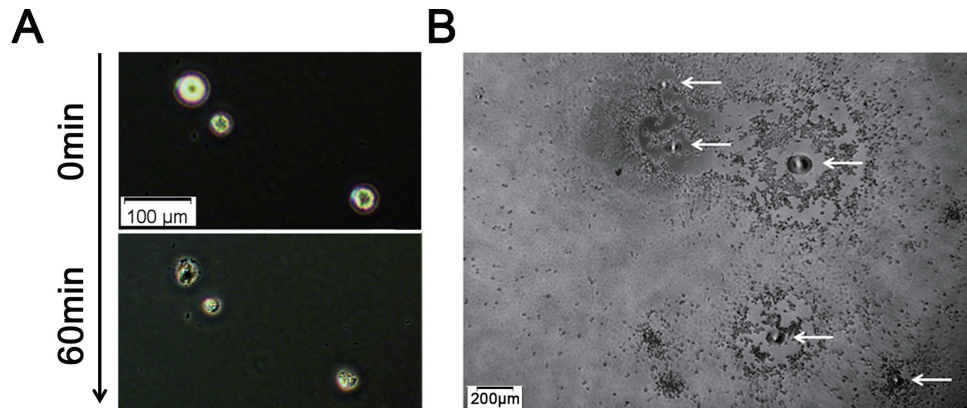


Fig. 3. The feature and toxic effects of CEES droplets. (A) The feature of CEES droplets on the glass surface was recorded at 0 min and 60 min, respectively. (B) Cells were exposed to 0.5 mM CEES freshly prepared in MEM containing 1 mg/mL PL-TG. After 3 hr exposure, the feature of droplets-injured cells under a microscope was captured. White arrows indicated CEES droplets.

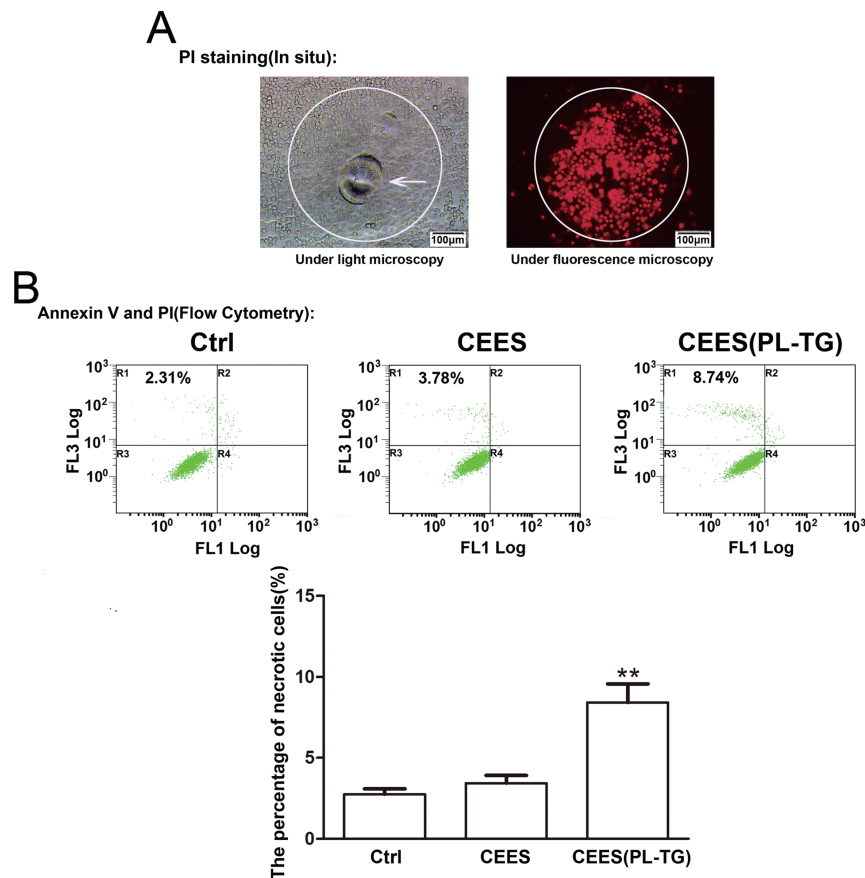


Fig. 4. CEES droplets increased the percentage of necrotic cells. (A) Cells were exposed to 0.5 mM CEES freshly prepared in MEM containing 1 mg/mL PL-TG. After 3 hr exposure, cells were stained with PI, and the necrotic cells were captured under a fluorescence microscope. White arrow indicated CEES droplets. The circle outlined CEES droplet-damaged area. (B) Flow cytometry was employed to separate and calculate the necrotic cells stained with Annexin V and PI. R1, necrotic cells; R2, late apoptotic cells; R3, normal cells; R4, early apoptotic cells. The typical image and the calculated results were shown. **, $P < 0.01$, compared to the control group ($n=4$).

er than that in the control group (Fig. 4B). These results indicated that CEES droplets were fatal to nearby cells, which led to cell necrosis, but not apoptosis.

CEES droplets decreased MMP from nearby cells

In situ study, CEES droplets were proved to decrease cellular MMP in a limited circle area. In this area, cells stained with JC-1 exhibited intense green fluorescences. Cells outside the damaged area exhibited a normal MMP (Fig. 5A). Additionally, using flow cytometry, we detected the percentage of MMP-declining cells in the PL-TG group was higher than that in the control group (Fig. 5B). Due to the importance of MMP in maintaining cell survival, MMP decline might play an essential role in CEES

droplets-induced cell necrosis.

DISCUSSION

It is known that sulfur mustard or its analog CEES has a higher specific density than water, and the very low solubility (0.1% at 30°C) leads to undissolved mustard fall into the bottom of the water. Vortex may disperse CEES into fine droplets as a solution status and enhance CEES solubility and hydrolysis in water. However, residual CEES droplets are hard to be avoided under the conventional solution preparation, such as diluting CEES in medium containing fetal serum (data not shown). In the present study, we showed that PL and TG, two essential components in serum, could promote CEES droplets for-

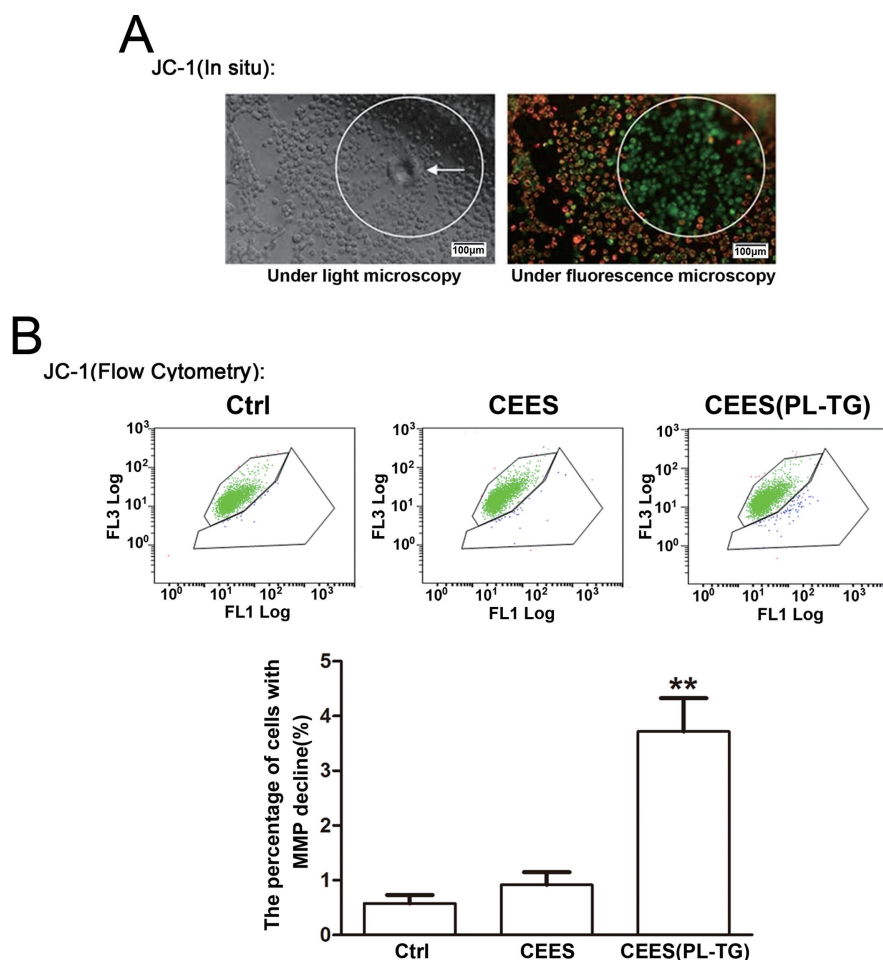


Fig. 5. CEES droplets increased the percentage of cells with MMP decline. (A) Cells were exposed to 0.5 mM CEES freshly prepared in MEM containing 1 mg/mL PL-TG. After 3 hr exposure, cells were stained with JC-1, and the fluorescent signal was captured under fluorescence microscopy. (B) For calculation, cells were digested and stained with JC-1, which were further detected using flow cytometry. FL1 and FL3 channels were set for separating normal (green) and MMP-declining cells (blue). The typical image and the calculated results were shown. **, $P < 0.01$, compared to the control group (n=4).

mation after the regular dilution and vortex of CEES solution. These findings may add our understanding of oily mustard droplets formation *in vitro* tests.

Until now, many methods have been constructed for SM biomarkers detection, such as the hydrolysis/oxidation products, β -lyase metabolites, DNA adducts, and hemoglobin adducts (Manandhar *et al.*, 2018; Zubeil *et al.*, 2019). However, the prototype of SM or CEES is hard to be detected as they are highly active and unstable once dissolving in water. Potassium thioacetate (PTA) can react with the dissolved SM to form a stable derivative, which had been reported recently in quantifying SM level (Xu *et al.*, 2015; Xu *et al.*, 2017). Based on this principle of chemical reaction, we completed CEES level detection by using the HPLC-UV system. Moreover, our method is simple without the use of a mass spectrometer. Results showed that CEES level was high at the beginning but significantly decreased to 30% after 3 min. The result is similar to other reports that the half-life of CEES in aqueous solution is in 2 min (Noort *et al.*, 2002; Tewari-Singh *et al.*, 2010). Moreover, we found that PL-TG partially blocked CEES conversion at 3 min and 9 min (not latter), indicating that CEES droplets might slowly dissolve in water. Since CEES is a lipophilic agent that may combine with PL and TG, the residual CEES droplets could be a result of the decreased solubility of CEES-PL-TG mixtures in water. Besides, due to the different character of PL (solid) and TG (oil), the complex treatment may have synergy effects on droplets formation. Further studies need to take to explore these questions.

The original feature of CEES droplet on glass was round with intense refraction, but changed to be irregular with weak refraction after 60 min, probably caused by hydrolysis and diffusion. In cultured cells, CEES droplets focally damaged nearby cells with MMP decline in a circular area. Since CEES (over 1.5 mM) in the medium can decline cellular MMP (Gould *et al.*, 2009), we assume that a high level of CEES existing in the circle area after CEES droplet diffusion, which severely damaged the contacted cells. Noticeably, the hallmark of necrosis, in general, is ATP deletion, as apoptosis requires a sufficient presence of intracellular ATP (Paromov *et al.*, 2011). Thus, we believe that CEES droplets-declined cellular MMP results of cell necrosis.

It should be noted that the general preparation of CEES solution is still feasible in exploring the molecular toxicity mechanism, even a bit of CEES droplets remaining, as most of the cells are out of CEES droplets-damaged area. Meanwhile, most of CEES droplets-damaged cells are detached from the culture plate, which can be removed after sufficient wash with PBS prior to harvesting cells.

After all, since the damage pattern of CEES droplet is different from that of the dissolved CEES *in vitro* condition, special attention on its formation and toxicity is still meaningful.

ACKNOWLEDGMENTS

This research was supported by the National Natural Science Foundation of China (grant number 81502711), the Major Military Medical S & T Project of PLA for the "Twelfth Five-year Plan" (AWS11C004), and the Natural Science Foundation of Chongqing (cstc2015jcyjA100-75).

Conflict of interest---- The authors declare that there is no conflict of interest.

REFERENCES

- Allon, N., Chapman, S., Shalem, Y., Brandeis, R., Weissman, B.A. and Amir, A. (2010): Lipopolysaccharide induced protection against sulfur mustard cytotoxicity in RAW264.7 cells through generation of TNF- α . *J. Toxicol. Sci.*, **35**, 345-355.
- Balali-Mood, M., Riahi-Zanjani, B., Mahmoudi, M. and Sadeghi, M. (2019): Current status of the acquired immune system of Iranian patients with long-term complications of sulfur mustard poisoning. *Daru*, **27**, 43-48.
- Deppe, J., Popp, T., Egea, V., Steinritz, D., Schmidt, A., Thiermann, H., Weber, C. and Ries, C. (2016): Impairment of hypoxia-induced HIF-1 α signaling in keratinocytes and fibroblasts by sulfur mustard is counteracted by a selective PHD-2 inhibitor. *Arch. Toxicol.*, **90**, 1141-1150.
- Gould, N.S., White, C.W. and Day, B.J. (2009): A role for mitochondrial oxidative stress in sulfur mustard analog 2-chloroethyl ethyl sulfide-induced lung cell injury and antioxidant protection. *J. Pharmacol. Exp. Ther.*, **328**, 732-739.
- Khazdair, M.R. and Boskabady, M.H. (2019): Long term effect of sulfur mustard exposure on hematologic and respiratory status, a case control study. *Drug Chem. Toxicol.*, **42**, 295-299.
- Manandhar, E., Pay, A., Veress, L.A. and Logue, B.A. (2018): Rapid analysis of sulfur mustard oxide in plasma using gas chromatography-chemical ionization-mass spectrometry for diagnosis of sulfur mustard exposure. *J. Chromatogr. A*, **1572**, 106-111.
- Noort, D., Benschop, H.P. and Black, R.M. (2002): Biomonitoring of exposure to chemical warfare agents: a review. *Toxicol. Appl. Pharmacol.*, **184**, 116-126.
- Panahi, Y., Abdolghaffari, A.H. and Sahebkar, A. (2018): A review on symptoms, treatments protocols, and proteomic profile in sulfur mustard-exposed victims. *J. Cell. Biochem.*, **119**, 197-206.
- Paromov, V., Brannon, M., Kumari, S., Samala, M., Qui, M., Smith, M. and Stone, W.L. (2011): Sodium pyruvate modulates cell death pathways in HaCaT keratinocytes exposed to half-mustard gas. *Int. J. Toxicol.*, **30**, 197-206.
- Price, C.C. and Bullitt, O.H. Jr. (1947): Hydrolysis and oxidation of mustard gas and related compounds in aqueous solution. *J. Org. Chem.*, **12**, 238-248.
- Rose, D., Schmidt, A., Brandenburger, M., Sturmheit, T., Zille, M. and Boltze, J. (2018): Sulfur mustard skin lesions: A system-

- atic review on pathomechanisms, treatment options and future research directions. *Toxicol. Lett.*, **293**, 82-90.
- Sezigen, S., Ivelik, K., Ortatatli, M., Almacioglu, M., Demirkasimoglu, M., Eyison, R.K., Kunak, Z.I. and Kenar, L. (2019): Victims of chemical terrorism, a family of four who were exposed to sulfur mustard. *Toxicol. Lett.*, **303**, 9-15.
- Shakarjian, M.P., Heck, D.E., Gray, J.P., Sinko, P.J., Gordon, M.K., Casillas, R.P., Heindel, N.D., Gerecke, D.R., Laskin, D.L. and Laskin, J.D. (2010): Mechanisms mediating the vesicant actions of sulfur mustard after cutaneous exposure. *Toxicological sciences: an official journal of the Society of Toxicology.*, **114**, 5-19.
- Steinritz, D., Weber, J., Balszuweit, F., Thiermann, H. and Schmidt, A. (2013): Sulfur mustard induced nuclear translocation of glyceraldehyde-3-phosphate-dehydrogenase (GAPDH). *Chem. Biol. Interact.*, **206**, 529-535.
- Tewari-Singh, N., Gu, M., Agarwal, C., White, C.W. and Agarwal, R. (2010): Biological and molecular mechanisms of sulfur mustard analogue-induced toxicity in JB6 and HaCaT cells: possible role of ataxia telangiectasia-mutated/ataxia telangiectasia-Rad3-related cell cycle checkpoint pathway. *Chem. Res. Toxicol.*, **23**, 1034-1044.
- Xu, B., Zong, C., Nie, Z., Guo, L. and Xie, J. (2015): A novel approach for high sensitive determination of sulfur mustard by derivatization and isotope-dilution LC-MS/MS analysis. *Talanta*, **132**, 245-251.
- Xu, B., Zong, C., Zhang, Y., Zhang, T., Wang, X., Qi, M., Wu, J., Guo, L., Wang, P., Chen, J., Liu, Q., Xu, H., Xie, J. and Zhang, Z. (2017): Accumulation of intact sulfur mustard in adipose tissue and toxicokinetics by chemical conversion and isotope-dilution liquid chromatography-tandem mass spectrometry. *Arch. Toxicol.*, **91**, 735-747.
- Zubel, T., Hochgesand, S., John, H., Steinritz, D., Schmidt, A., Burkle, A. and Mangerich, A. (2019): A mass spectrometric platform for the quantitation of sulfur mustard-induced nucleic acid adducts as mechanistically relevant biomarkers of exposure. *Arch. Toxicol.*, **93**, 61-79.